

1 **Modelling and testing the performance of a commercial ammonia/water**  
2 **absorption chiller using Aspen-Plus platform**

3  
4  
5 **Rami Mansouri**<sup>a,b</sup>, **Ismail Boukholda**<sup>a</sup>, **Mahmoud Bourouis**<sup>b\*</sup>, **Ahmed Bellagi**<sup>a</sup>  
6  
7

8 <sup>a</sup> *U.R. Thermique et Thermodynamique des Procédés Industriels*  
9 Ecole Nationale d'Ingénieurs de Monastir (ENIM), University of Monastir - Tunisia  
10

11 <sup>b</sup> Department of Mechanical Engineering – Universitat Rovira i Virgili,  
12 Tarragona - Spain.  
13

14  
15 \*Corresponding author

16 Email: [mahmoud.bourouis@urv.cat](mailto:mahmoud.bourouis@urv.cat) ; Phone: +34 977 55 86 13 ; Fax: +34 977 55 96 91  
17  
18

19 **Abstract**

20 A steady-state simulation model of a commercial 3-ton ammonia/water absorption chiller is  
21 developed and validated using the flow-sheeting software Aspen-Plus. First an appropriate  
22 thermodynamic property model for the ammonia/water fluid mixture is selected. To this  
23 purpose nine methods from the software library are pre-selected and tested, but none of the  
24 methods predicts the vapour-liquid equilibrium (VLE) with sufficient accuracy. The  
25 interaction parameters of these models are then determined by fitting the equations of state  
26 (eos) to VLE data. It is finally found that the Boston-Mathias modified Peng-Robinson eos  
27 with fitted parameters predicts most accurately the VLE for the temperature and pressure  
28 ranges encountered in commercial chillers.

29 A simulation model of the machine is then developed. The simulation results are found to be  
30 in good agreement with data from literature at a cooling air temperature of 35 °C. The heat  
31 transfer characteristics (*UA*) of the various heat exchangers of the machine are then  
32 determined and the model modified to make it accept these (*UA*) as input parameters. The

33 comparison of the simulation predictions at cooling air temperatures of 26.7 and 38 °C with  
34 the bibliographical data showed good concordance. The proposed model could be very useful  
35 for the analysis and prediction of the performances of the commercial chiller.

36 **Keywords:** Absorption refrigeration, ammonia/water, thermodynamic property model, Aspen-  
37 Plus, Robur.

---

### 38 **Highlights**

- 39 ○ A commercial NH<sub>3</sub>/H<sub>2</sub>O absorption chiller is simulated using the software Aspen-Plus.
- 40 ○ Peng-Robinson-Boston-Mathias equation of state is used to predict VLE of NH<sub>3</sub>/H<sub>2</sub>O  
41 fluid mixture.
- 42 ○ A steady-state model describing the chiller operation is developed.
- 43 ○ The model predicts the internal operating conditions and *COP* of the chiller.  
44  
45

## 46 **1. Introduction**

47 Due to the rapid increase in global demand for energy and the need to reduce greenhouse gas  
48 emissions, the interest in finding new efficient ways of using energy is growing. Cooling  
49 technologies are of great economical, energetic and environmental importance. The  
50 conventional vapour compression refrigeration and air conditioning systems are driven by  
51 electrical energy which consumes worldwide huge amounts of this kind of energy and also  
52 contributes to the greenhouse effect in the atmosphere. Priority should be given to the  
53 investigation and use of alternative driving energy sources instead of electricity for cooling  
54 applications. The interest is focused on absorption cooling technology as it is an attractive  
55 alternative and sustainable solution to replace vapour compression units. Indeed, waste heat  
56 rejected in many industries is at higher temperatures than the heat source temperatures  
57 required for driving most of the absorption cooling systems [1-3]. The use of thermally driven  
58 cooling systems can help in reducing problems related to global warming, such as the green-  
59 house effect due to CO<sub>2</sub> emissions from the combustion of fossil fuels in thermal power  
60 plants. Also the common refrigerant/absorbent working fluids, namely water/lithium bromide  
61 and ammonia/water, used in absorption cooling systems are both environment-friendly.  
62 Nowadays, several studies are focused on finding new ways to directly use thermal or solar  
63 energy to drive cooling machines. Investigations are being carried out on the development of  
64 new and hybrid cycle configurations and finding new potential working fluids.

65 Lazzarin *et al.* [4] reported a detailed work on a gas-fired 5 tons ammonia/water absorption  
66 chiller for refrigeration applications. The authors studied the performance of the chiller by  
67 modifying its initial charge and proposed some modifications on the machine to produce cold  
68 at temperatures as low as -25°C. Chua *et al.* [5] presented a general framework for  
69 thermodynamic modelling of an irreversible absorption chiller focusing on the design and  
70 tested their theoretical approach on a single-stage ammonia/water unit. Component models of

71 the chiller have been assembled so as to quantify the internal entropy production and thermal  
72 conductance ( $UA$ ) in a thermodynamically rigorous formalism, which is in agreement with the  
73 simultaneous heat and mass transfer processes occurring within the exchangers. Local  
74 thermodynamic balances (energy, entropy and mass balances) and consistency within the  
75 components are respected, in addition to the overall thermodynamic balance as determined by  
76 the inlet and outlet states of the components. For the absorbers, Colburn-and-Drew mass  
77 transfer equations are incorporated to describe the absorption process. Furthermore, the  
78 impact of various irreversibilities on the performance of chiller is also evaluated through the  
79 use of a general macroscopic equation. Horuz and Callander [6] carried out experimental  
80 investigations on the 3 tons Robur gas-fired chiller and studied the response of the system to  
81 variations of the chilled water flow rate, inlet temperature and level in the evaporator drum for  
82 variable heat inputs by modifying the air-cooled components (a water-cooled absorber and a  
83 water-cooled condenser units were incorporated into the system in order to test the  
84 experimental system under wider range of condenser and absorber pressures). Darwish *et al.*  
85 [7] analysed the Robur absorption refrigeration water/ammonia (ARWA) system using the  
86 Aspen-Plus simulator. The results were compared with some manufacturer compiled data  
87 reported in the open literature. The performance parameters employed for the analysis were:  
88 coefficient of performance ( $COP$ ), heat duties of the evaporator, absorber and condenser,  
89 concentration in the ammonia poor and ammonia rich solutions, and flow rates of the  
90 ammonia poor solution and refrigerant vapour leaving the evaporator. Agreement between the  
91 simulation results and the experimental measurements was observed. Some innovative  
92 modifications in the Robur cycle aimed at enhancing the generator operation showed a  
93 significant improvement in the  $COP$ . In particular, introducing a throttling process directly  
94 prior to the generator could alleviate the generator heat load and enhance the  $COP$  up to 20%.  
95 Rossa and Bazzo [8] investigated theoretically the feasibility of a small-scale cogeneration

96 system for cold and electricity production. The system consisted of a 5-ton Robur absorption  
97 chiller and a 28 kWe natural gas micro-turbine whose exhaust gas was used to drive the  
98 absorption chiller. The authors reported a thermal efficiency of 41 % for the combined  
99 cooling and power system, which in turn represents an enhancement of 67% in the efficiency  
100 of a single natural-gas micro-turbine. El May *et al.* [9] developed a modular simulation  
101 program under Mathematica for absorption heat pumps, refrigerators and air conditioners. The  
102 modular approach is an easier way to simulate various complex configurations. As an  
103 application, the commercial Robur absorption machine was studied. The predicted results  
104 showed well agreement with experimental data from the open literature. El May *et al.* [10]  
105 presented and discussed the results of an energetic and exergetic analysis of a commercial air-  
106 cooled water/ammonia absorption machine with a cooling capacity of 10 kW. The comparison  
107 with a conventional single-effect absorption chiller operating under the same conditions  
108 showed that to achieve similar performances to those of the pre-absorber in the Robur chiller,  
109 an additional heat transfer area in the air-cooled absorber was required to ensure the complete  
110 absorption of the refrigerant. The second law analysis revealed that the highest exergy  
111 dissipation (75 %) is located in the driving compartment and that the irreversible absorption  
112 process was responsible for an important part (45%) of the *COP* degradation.

113 In the present work, a steady-state simulation model is developed using the Aspen-Plus  
114 platform to test and analyse the performance of a commercial 3-ton gas-fired absorption  
115 chiller (10 kW cooling capacity) at different operating conditions. This air-conditioner uses  
116 ammonia/water as a working fluid. This particular chiller has been chosen in this study for the  
117 following reasons:

- 118 i. Although absorption technique is used for cold production, its thermodynamic cycle  
119 presents some particularities and complex flow connections in comparison with

120 conventional absorption machines. In particular a solution cooled absorber, called pre-  
121 absorber, is incorporated in the Robur chiller to improve its performances;

122 ii. There is scarce information in the open literature on how to choose an appropriate  
123 thermodynamic property model for the ammonia/water mixture to simulate absorption  
124 chillers and heat pumps in Aspen-Plus [11];

125 iii. The absorption chiller is a commercial unit and operational experimental data is  
126 available in the open literature.

## 127 **2. Chiller description and working principles**

128 A schematic representation of the Robur absorption machine is shown in Figure 1. In the  
129 generator, the ammonia/water mixture is heated by thermal energy input provided from a gas  
130 burner to desorb the refrigerant. The refrigerant vapours (12) flow to the rectifier where they  
131 are cooled by the ammonia rich solution on its way to the generator and which is thus  
132 preheated. This causes partial condensation of the water vapours purifying further the  
133 ammonia vapours. These flow to the air-cooled condenser where they are liquefied. The liquid  
134 refrigerant (8) circulates then to the refrigerant heat-exchanger and further to the refrigerant  
135 expansion valve. After reduction of its pressure, the refrigerant is introduced in the evaporator  
136 (10) where it evaporates by absorbing heat from the chilled water. The refrigerant vapour  
137 flows to the absorber where it is absorbed by the ammonia poor solution returning from the  
138 generator in two steps: first, in the pre-absorber where the absorption heat released is used to  
139 preheat the ammonia rich solution on its way to the generator (4) and then in the air-cooled  
140 absorber to complete the absorption process. 3D-Sketches of the internal view of the machine  
141 and its components are presented in Appendix 1 (Figs 12 and 13).

### 142 3. Aspen-Plus modelling approach

#### 143 3.1 Thermodynamic property models

144 Ammonia/water mixture has been used as a working fluid in absorption refrigeration systems  
145 for several decades. To simulate an absorption refrigeration cycle, the thermo-physical  
146 properties of the working fluid play a vital role [12]. Different equations are available in the  
147 literature [13-25] to calculate the thermodynamic properties of ammonia/water system: Virial  
148 equations of state, cubic equations of state, Polynomial functions, Helmholtz free energy,  
149 Perturbation theory and Gibbs excess energy.

150 Schulz [22] presented a fundamental equation of state for this binary mixture. Ziegler and  
151 Trepp [23] modified the Schulz equation of state and developed new correlations for  
152 predicting the equilibrium properties required in the analysis of absorption refrigeration  
153 cycles. The authors used the Gibbs excess energy equation to determine specific volume,  
154 specific entropy and specific enthalpy. Using the new correlation, the thermodynamic  
155 properties can be predicted up to a pressure of 50 bars and a temperature of 500 K. Renon *et*  
156 *al.* [13] derived an equation of state which can accurately estimate the properties of  
157 ammonia/water mixtures. An extended Redlich-Kwong equation of state with two adjustable  
158 parameters was used to predict VLE of the working fluid. Ruiter [24] presented a simplified  
159 thermodynamic model for the mixture. The equilibrium pressure and the excess enthalpy of  
160 the gas and liquid phases were described using 11 coefficients. Patek and Klomfar [15]  
161 presented five equations to predict VLE properties. The use of these equations avoids iterative  
162 procedures when calculating thermodynamic properties of ammonia/water mixture. The  
163 equations were developed by fitting critically assessed experimental data using simple  
164 functional forms. The results were presented in form of an enthalpy-concentration diagram.  
165 Barhoumi *et al.* [21] reported a detailed work on the reformulation of the thermodynamic

166 properties of the ammonia/water mixture using the Gibbs energy function. For the liquid  
167 phase, a three constant Margules model of the excess free enthalpy was formulated. The  
168 vapour phase was considered a perfect mixture of real gases, each pure gas being described by  
169 a virial equation of state in pressure truncated after the third term. The model developed  
170 predicts the thermodynamic properties of the mixture with great accuracy in the three states,  
171 i.e. subcooled liquid, superheated vapour and liquid-vapour saturation in the temperature  
172 range of 200 to 500 K and a pressure up to 100 bars.

173 Mejbri and Bellagi [25] modelled the thermodynamic properties of the ammonia/water  
174 mixture using three different approaches: An empirical Gibbs free enthalpy model, the Patel-  
175 Teja cubic equation of state and the PC-SAFT (Perturbed Chain Statistical Associating Fluid  
176 Theory) equation of state. A comparison of these three methods proved the superiority of the  
177 PC-SAFT equation of state to predict and extrapolate the thermodynamic properties of  
178 ammonia/water system over a larger range of temperature ( $273.16 \leq T \leq 613.15$  K) and  
179 pressure ( $0 < P \leq 210$  bar). Also, the authors recommended the use of the Gibbs free enthalpy  
180 model for industrial applications that use ammonia/water as a working fluid at moderate  
181 temperatures and pressures, such as absorption refrigeration.

182 The selection of a proper method for estimating the thermodynamic properties of the working  
183 fluid is one of the most important steps that can affect the simulation of absorption  
184 refrigeration cycles. Therefore, it is important to choose carefully an appropriate method to  
185 estimate the different properties of the working fluid. Aspen-Plus includes a large databank of  
186 thermodynamic property and transport models with the corresponding mixing rules for  
187 estimating the mixture properties. Before performing a simulation in Aspen-Plus, it is  
188 important to ensure that the selected property method is the best reliable thermodynamic  
189 model. In this work, the choice of the ammonia/water mixture property model for use in the  
190 simulation of the gas-fired chiller is investigated in detail. To this purpose the predictions of

191 the nine property models available in Aspen-Plus for this working fluid are evaluated and  
192 compared with regressed experimental vapor-liquid equilibrium data reported by Mejbri and  
193 Bellagi [25] in the pressure range from 2 to 25 bar and the temperature range from -19 to 220  
194 °C. In a second step, the Aspen-Plus Data Regression System facility is used to fit the  
195 interaction parameters of the property models to the VLE data of reference [25]. The results  
196 are presented in the form of  $T$ - $x$ - $y$  diagrams.

### 197 **3.2 Selection of the thermodynamic property model**

198 The nine property models implemented in Aspen-Plus and considered for the calculation of  
199 the properties of the ammonia/water mixture are listed in Table 1. This list includes cubic eos  
200 methods (SRK, PR-WS and PR-MHV2, PENG-ROB, PR-BM, RKS-BM) as well as activity  
201 coefficient methods (ENRTL-RK, NRTL-HOC, WILS-RK). The tests of these models are  
202 performed in two steps. In the first one,  $T$ - $x$ - $y$  VLE prediction by each of the Aspen-Plus  
203 property models are compared with the regressed data reported in [25] for 6 isobars, namely  
204 2, 4, 10, 16, 20 and 25 bars. Figures 2, 3 and 4 illustrate this comparison for 2, 10 and 25 bar,  
205 respectively. It is observed that the maximum equilibrium temperature deviation predicted by  
206 the considered nine property models implemented in Aspen-Plus and the data reported by  
207 Mejbri and Bellagi [25] is about 10 °C. As regards the ammonia mass fraction in the liquid  
208 phase, the values predicted by the property models SRK, PR-WS and PR-MHV2 are  
209 inconsistent in the whole pressure range. This is the case also of the three activity coefficient  
210 models (ENRTL-RK, NRTL-HOC, WILS-RK) for the pressures 10 and 25 bars, for which the  
211 deviations increase with increasing pressure. It is concluded that none of these property  
212 models reproduces the ammonia/water vapour-liquid equilibrium data with sufficient  
213 accuracy.

214 In a second step, the data regression system of Aspen-Plus was used to fit the parameters of  
215 the property models by using the VLE data reported by Mejbri and Bellagi [25]. For the cubic  
216 equations of state it is the interaction parameter  $k_{ij}$  — or its coefficients  $k_{ij}^{(1)}, k_{ij}^{(2)}, k_{ij}^{(3)}$  if it is  
217 supposed temperature dependent (see Appendix 2 for details) — that are fitted to the VLE  
218 data. Figures 5, 6 and 7 show the corresponding comparison for 2, 10 and 25 bars,  
219 respectively. As can be noted, all values of the ammonia mass fraction in the vapour phase  
220 predicted by the Aspen-Plus property models are now close to the data reported by Mejbri and  
221 Bellagi [25]. Regarding the ammonia mass fraction in the liquid phase, the PR-MHV2 model  
222 made the poorest predictions. These figures make also clear that the PR-BM model (Peng-  
223 Robinson eos with Boston-Mathias alpha function, see Appendix for details) is in better  
224 agreement with the considered vapour-liquid equilibrium data. The sum of squared errors for  
225 the nine Aspen-Plus property models tested and summarized in Table 2 confirms this  
226 conclusion. This table shows also that with the help of data regression eight of the nine  
227 property models have been successfully fitted to make them predict VLE close to the  
228 experimental data. Just one property model fails to accommodate well the data: PR-MHV2. It  
229 is concluded from these results that the Peng-Robinson-Boston-Mathias equation of state (PR-  
230 BM), with fitted parameters, is the most appropriate property method among those  
231 implemented in Aspen-Plus for the prediction of the ammonia/water vapour-liquid  
232 equilibrium in the investigated temperature and pressure ranges. Table 3 gives the default and  
233 regressed values of the parameters  $k_{ij}^{(1)}, k_{ij}^{(2)}$  and  $k_{ij}^{(3)}$  for the considered cubic equation of  
234 state.

### 235 3.3 State points and assumptions

236 The steady-state simulation model developed in the present work using the flow-sheeting  
237 software Aspen-Plus is intended to analyse the performance of the air-cooled Robur

238 absorption chiller investigated experimentally by Klein [26]. This author carried out his  
239 experiments in an environmental chamber at three cooling air temperatures, namely 26.7°C,  
240 35°C and 38°C, with 14 temperature measurement points in the chiller.

241 The analysis presented in the present paper is performed in two steps. Firstly, the heat transfer  
242 characteristics of the major heat exchanging devices of the machine: condenser, evaporator,  
243 absorber and refrigerant heat exchanger are deduced from operating data of the chiller at a  
244 cooling air temperature of 35 °C. This heat exchanger characteristic, the heat conductance,  
245 sometimes referred to as the heat capacity of the heat exchanger, is generally defined by the  
246 equation

$$\dot{Q} = (UA)\Delta T_{ln}$$

247 Where  $\dot{Q}$  is the heat duty and  $\Delta T_{ln}$  the logarithmic mean temperature difference, LMTD, at  
248 the hot (subscript,  $h$ ) and cold (subscript,  $c$ ) ends of the exchanger,

$$\Delta T_{ln} = \frac{(T_{h,i} - T_{c,o}) - (T_{h,o} - T_{c,i})}{\ln \left[ \frac{(T_{h,i} - T_{c,o})}{(T_{h,o} - T_{c,i})} \right]}$$

249 With the subscripts  $i$  and  $o$  referring to inlet and outlet, respectively.

250 The simulations results are then compared with experimental data of Klein [26] and those  
251 obtained by simulation of El May *et al.* [10]. In a second step, the model is then modified to  
252 include the  $(UA)$  values of the heat exchangers determined in the previous step as input  
253 parameters. The results are compared with the two sets of data from the literature [10, 26] at  
254 cooling air temperatures of 26.7°C and 38°C.

255 Figure 8 shows the Robur model in Apen-Plus. The state points in the chiller are defined as  
256 follows. The absorber exit is state point 1A which also represents the inlet of the solution

257 pump at state point 1; the pump exit is state point 2. State point 5 represents the rectifier exit;  
258 the pre-absorber exit leading to the generator is state point 4; the solution exit of the generator  
259 leading to valve 2 is state point 6; the valve 2 exit leading to the pre-absorber is state point 3.  
260 The vapour exit of the generator is state point 7; the condenser exit is state point 8. The  
261 refrigerant heat exchanger exit leading to valve 1 is state point 13; the refrigerant valve exit is  
262 state point 9. The evaporator exit is state point 10; the refrigerant heat exchanger exit leading  
263 to the pre-absorber is state point 11, and the pre-absorber exit leading to the absorber is state  
264 point 14. The model assumptions and calculation sequence for the chiller simulation at a  
265 cooling air temperature of 35 °C are summarized in Table 4.

### 266 **3.4 Model components**

267 Modelling a process in Aspen-Plus is based on the appropriate selection of the equivalent  
268 blocks for the main components to build a running model. Table 5 gives the Aspen blocks for  
269 the various machine elements as well as the input data for these elements for the 35 °C  
270 cooling air temperature case. The models for the pump and the two expansion valves are  
271 obvious. The default value of pump efficiency (100%) is used, as the effect of this parameter  
272 on the overall cycle performance is negligible. For the air-cooled condenser and absorber, the  
273 evaporator and the solution heat exchanger a two-flow heat exchanger model is used. For the  
274 separation of the refrigerant in the generator a multi-stage rectification column with condenser  
275 and boiler is needed. For the pre-absorber a simplified model combining a flash tank and a  
276 heater is adapted to account for the complex heat and mass transfer processes taking place in  
277 this machine element: On one side, hot ammonia poor solution from the generator is mixed  
278 with cold refrigerant vapours coming from the evaporator, resulting in a partial absorption and  
279 a liquid/vapour mixture leaving for the air-cooled absorber, and on other side, ammonia rich  
280 solution on its way to the generator preheated by the hot ammonia poor solution and by the  
281 heat released resulting from the partial absorption process.

282 Finally, the cooling medium air is modeled as gas mixture with 78 % Nitrogen by mole, 21 %  
283 Oxygen by mole and 1 % Argon by mole.

### 284 **3.5 Simulation procedure**

285 The simulation model developed in the present work uses in a first step a sequential modular  
286 approach in which each block is calculated separately. A “break point” is considered in the  
287 model for the cycle input conditions. This “break” point is inserted at state point 1, the  
288 solution pump inlet (Figure 8). The exit of the absorber (state point 1A) and the inlet of the  
289 solution pump (state point 1) represent the same state, and consequently state point 1A should  
290 have the same characteristics as those given as inputs at the solution pump inlet after the  
291 simulations are run. This constitutes the convergence criterion for the simulations.

292 As Equation Oriented Modelling is a more effective way of solving of complex problems, the  
293 simulations are run, in a second step, using the Equation-Oriented (EO) approach: the  
294 governing equations of the chiller model are solved simultaneously. To reach convergence in  
295 this approach, good initial estimates for all variables are necessary. A good practice is then to  
296 begin the simulation in sequential modular mode and to initialize (synchronize) the EO  
297 solution procedure using the results of the sequential simulation after complete convergence.

## 298 **4. Results and discussion**

### 299 **4.1 Heat transfer characteristics of the main thermal components of the chiller**

300 As mentioned previously the start input values are introduced into the chiller simulation  
301 considering a "break" point at state point 1. A well-formulated model will conserve mass and  
302 energy throughout the cycle, thus resulting in identical characteristics of the flows on either  
303 side of the break 1A. The cycle state points resulting from the Aspen-Plus model at a cooling  
304 air temperature of 35 °C are given in Table 6. The experimental data reported by Klein [26]

305 and the simulation results obtained by El May *et al.* [10] are used to validate our Aspen-Plus  
306 model. The validation parameters employed are: driving heat input, coefficient of  
307 performance (*COP*) and temperature measured by Klein [26] at 14 locations in the chiller.  
308 Table 7 shows the thermal loads in the main components and the *COP* of the absorption  
309 chiller reported by Klein [26] and the values obtained in the present work. As regards the  
310 thermal loads, the maximum deviation is observed in the driving heat in the generator which  
311 is less than 7%. The deviation obtained in the *COP* is about 5%. In Figure 9, the temperature  
312 values measured experimentally by Klein [26] are compared with the corresponding values  
313 obtained in the present work and those obtained by El May *et al.* [10] in their simulation. This  
314 comparison shows excellent agreement between the Aspen-Plus model results and Klein's  
315 data, except for state point 11 (refrigerant vapour leaving the refrigerant heat exchanger) for  
316 which the deviation is more than 10 °C. The results are also well in agreement with the  
317 simulation results obtained by El May *et al.* [10], except at 4 state points namely 4 (ammonia  
318 rich solution entering the generator), 13 (Refrigerant liquid leaving the refrigerant heat  
319 exchanger), 14 (ammonia poor solution entering the absorber) and 11 (refrigerant vapour  
320 leaving the refrigerant heat exchanger) for which the temperature deviation is higher than 5  
321 °C. The temperature values calculated in the present work and in El May *et al.* [10] for state  
322 point 11 are similar, which could mean that the experimental data from Klein [26] at this point  
323 is not of a good quality. The results commented above validate the model developed in  
324 Aspen-Plus for the Robur absorption chiller.

325 Next, the (*UA*) values were calculated for the condenser, evaporator, absorber and refrigerant  
326 heat exchanger (Table 8).

#### 327 **4.2 Model predictions with (*UA*) values as input parameters**

328 In this second step, the Aspen-Plus model for this particular absorption chiller is then  
329 modified to include the heat transfer capacities ( $UA$ ) of the condenser, evaporator, absorber  
330 and refrigerant heat exchanger – deduced from the simulation results at a cooling air  
331 temperature of 35 °C – as input parameters for the simulations at cooling air temperatures of  
332 26.7 °C and 38 °C. In Figure 10, the temperatures calculated using the Aspen-Plus model are  
333 compared with the experimental data from Klein [26] and simulated temperatures reported by  
334 El May *et al.* [10] at a cooling air temperature of 26.7 °C. The results obtained in the present  
335 work are well in agreement with both sets of data. In the case of comparison with  
336 experimental data from Klein [26], the maximum deviations are observed in state points 4  
337 (refrigerant vapour entering the generator) and 11 (refrigerant vapour leaving the refrigerant  
338 heat exchanger). Regarding the comparison with data obtained by El May *et al.* [10], the  
339 maximum deviation is observed in state point 14 (ammonia poor solution entering the  
340 absorber). Figure 11 shows the same comparison at a cooling air temperature of 38 °C. In  
341 general terms, the results of the present work are well in agreement with data from Klein [26]  
342 and El May *et al.* [10]. The maximum deviations are obtained in state points 7 (Refrigerant  
343 vapour entering the condenser), 11 (refrigerant vapor leaving the refrigerant heat exchanger)  
344 and 13 (Refrigerant liquid leaving the refrigerant heat exchanger) for the comparison with  
345 experimental data from Klein [26] and in state points 11, 13, 14 and 3 (ammonia poor solution  
346 entering the pre-absorber) for the comparison with simulated data from El May *et al.* [10]. It  
347 is worth mentioning that the temperature values calculated in the present work and in El May  
348 *et al.* [10] for state points 11 and 13 are similar, which could mean that the Klein [26]  
349 experimental data at these points is not of such a good quality. Table 9 shows a comparison  
350 between experimental temperature data [26], the simulation results of [10] and the model  
351 calculated temperatures at a cooling air temperature of 38 °C.

352 Based on these results, it is concluded that the version of the Aspen-Plus model that includes  
353 the ( $UA$ ) values of the condenser, evaporator, absorber and refrigerant heat exchangers as  
354 input parameters could be very useful for predicting the internal operating conditions and the  
355 coefficient of performance of the Robur absorption chiller at different temperatures of the  
356 cooling air and taking in account the real size of the heat exchangers.

## 357 **5. Conclusion**

358 In this paper, a steady-state model of a commercial 3-ton ammonia/water absorption chiller  
359 was developed using the flow-sheeting software Aspen-Plus. For the selection of the  
360 appropriate property model for the working fluid mixture, nine different models implemented  
361 in Aspen-Plus were evaluated in two steps. Firstly, calculated VLE by each of the Aspen-Plus  
362 property models was compared with regressed VLE data reported by Mejbri and Bellagi [25]  
363 at different pressures. It was concluded that none of these property models predicts the  
364 ammonia/water vapor-liquid equilibrium with sufficient accuracy. Secondly, the aspen-Plus  
365 data regression system was used to calculate the parameters of the Aspen-Plus property  
366 models by fitting the vapour-liquid equilibrium data reported by Mejbri and Bellagi [25]. It  
367 was found that the Peng-Robinson-Boston-Mathias equation of state (PR-BM) with regressed  
368 interaction parameters is the most suitable property model for the system water/ammonia in  
369 the temperature and pressure ranges encountered in absorption air-conditioning units.

370 Once the appropriate property model for ammonia/water mixture selected, an Aspen-Plus  
371 model was developed to simulate the steady-state operation of the commercial gas-fired  
372 chiller. First, the heat transfer characteristics of the condenser, evaporator, absorber and  
373 refrigerant heat exchanger were deduced from data at a cooling air temperature of 35 °C.  
374 Then, the results were compared with experimental data published by Klein [26] and those  
375 calculated by El May *et al.* [10]. The comparison showed good agreement between the

376 Aspen-Plus model results and the sets of data from the open literature. The model was then  
377 modified to include the ( $UA$ ) values of the heat exchangers calculated in the previous step as  
378 input parameters. The results were compared with the experimental data from Klein [26] and  
379 those reported by El May *et al.* [10] at cooling air temperatures of 26.7°C and 38°C. The  
380 results showed agreement with the two sets of bibliographical data. Therefore, it is concluded  
381 that the proposed Aspen-Plus model can be very useful tool for predicting the internal  
382 operating conditions and the coefficient of performance of the commercial gas-fired  
383 absorption chiller at different temperatures of the cooling air and taking in account the real  
384 size of the heat exchangers.

385

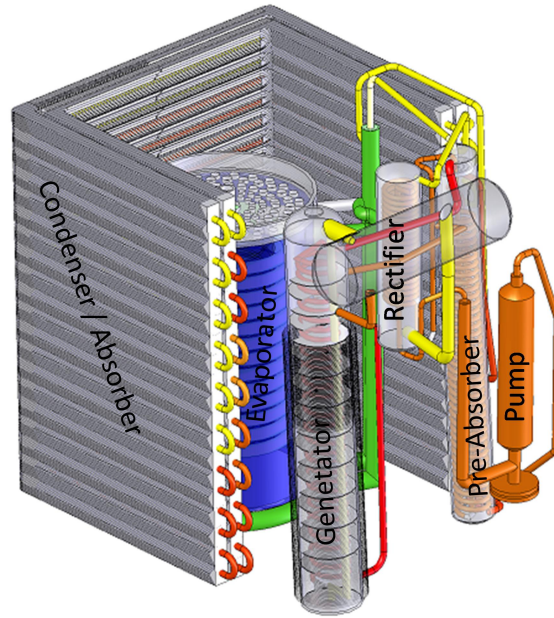
386

## Appendix 1

387

### Commercial 3-ton ammonia/water absorption chiller

388



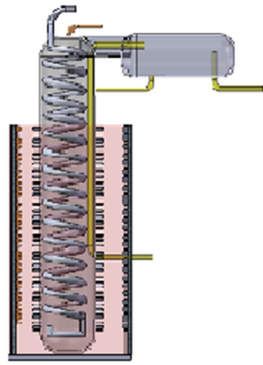
389

390

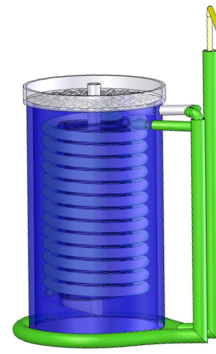
Figure12. Internal view of the commercial absorption chiller

391

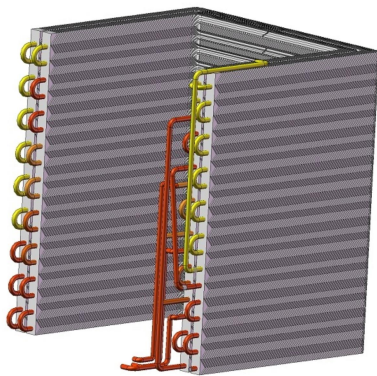
392



(a) Generator



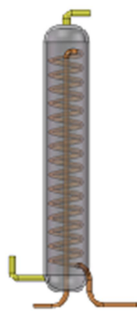
(b) Evaporator



(c) Absorber and Condenser



(d) Pre-absorber



(e) Rectifier



(f) Solution pump

393 Figure13. Schematic representation of the main components of the absorption chiller

394

395

396

397

## Appendix 2

398

### Peng-Robinson Equation of State

399 This cubic eos writes for mixtures [11, 27]:

$$P = \frac{RT}{(\bar{V} - b)} - \frac{a}{\bar{V}(\bar{V} + b) + b(\bar{V} - b)}$$

400 Where  $P$  is the pressure,  $\bar{V}$ , the mixture molar volume,  $b$ , the mixture co-volume,  $a$ , the401 attraction term factor, and  $R$  the universal gas constant. The mixture  $a$  and  $b$  are deduced402 from the individual component constants  $a_i$  and  $b_i$  using the mixing rules:

$$b = \sum x_i b_i$$

$$a = \sum_i \sum_j x_i x_j \sqrt{a_i a_j} (1 - k_{ij})$$

403 In these equations  $x_i$  is the mole fraction of component  $i$  in the mixture and  $k_{ij}$  the binary404 interaction parameter of components  $i$  and  $j$ . Usually it is supposed that:

$$k_{ij} = k_{ji}$$

405 It is this parameter that is deduced from VLE data by a regression procedure. To make the

406 equation more flexible  $k_{ij}$  is often written as function of the temperature:

$$k_{ij} = k_{ij}^{(1)} + k_{ij}^{(2)} T + \frac{k_{ij}^{(3)}}{T}$$

407 So that three parameters are fitted to the VLE data:  $k_{ij}^{(1)}$ ,  $k_{ij}^{(2)}$  and  $k_{ij}^{(3)}$ .408 The individual constants  $a_i$  and  $b_i$  are determined from the critical temperature and pressure409 of the compound,  $T_{ci}$  and  $P_{ci}$ , respectively:

$$a_i = \alpha_i(T) \left[ 0.45724 \frac{R^2 T_{ci}^2}{P_{ci}} \right]$$

$$b_i = 0.07780 \frac{RT_{ci}}{P_{ci}}$$

410 In the  $\alpha_i(T)$  function,

$$\alpha_i(T) = [1 + m_i(1 - \sqrt{T_r})]^2$$

411  $T_r$  is the reduced temperature,  $\frac{T}{T_{ci}}$ , and  $m_i$ , a component specific parameter depending on the

412 acentric factor  $\omega_i$ ,

$$m_i = 0.37464 + 1.54226 \omega_i - 0.26992 \omega_i^2$$

413  $\alpha_i(T) = 1$  at the critical temperature.

414 The Boston-Mathias modification of the Peng-Robinson equation of state is as follow:

$$\alpha_i(T) = \left[ \exp[c_i(1 - T_{ri}^{d_i})] \right]^2$$

415 with

$$d_i = 1 + \frac{m_i}{2} ; c_i = 1 - \frac{1}{d_i}$$

416 It's intended to extend the validity of the equation of state for temperatures larger than the

417 critical temperature. In fact, this is necessary for the water/ammonia mixture considered as a

418 working fluid in the absorption chiller because temperatures between 180 and 200°C are

419 needed in the generator to desorb the refrigerant. This temperature range is beyond the critical

420 temperature of ammonia (405.5 K corresponding to 132.4°C).

421

422 **References**

- 423 [1] Rodgers P., Mortazavi A., Eveloy V., Al-Hashimi S., Hwang Y., Radermacher R.  
424 Enhancement of LNG plant propane cycle through waste heat powered absorption  
425 cooling. *Applied Thermal Engineering*, 2012, 48, 41-53.
- 426 [2] Chan C.W., Ling-Chin J., Roskilly A.P. A review of chemical heat pumps,  
427 thermodynamic cycles and thermal energy storage technologies for low grade heat  
428 utilization. *Applied Thermal Engineering*, 2013, 53 (2), 160-176.
- 429 [3] El May S., Sayadi Z., Bellagi A. Feasibility of air-cooled solar air-conditioning in hot  
430 arid climate regions. *Int. J. of Sustainable Energy*, 2009, 28 (4), 183-193.
- 431 [4] Lazzarin R.M., Gasparella A., Longo G.A. Ammonia-water absorption machines for  
432 refrigeration: Theoretical and real performances. *Int. J. of Refrigeration*, 1996, 19 (4),  
433 239-246.
- 434 [5] Chua H.T., Toh H.K., Ng K.C. Thermodynamic modeling of an ammonia-water  
435 absorption chiller. *Int. J. of Refrigeration*, 2002, 25 (7), 896-906.
- 436 [6] Horuz I., Callander T.M.S. Experimental investigation of a vapor absorption refrigeration  
437 system. *Int. J. of Refrigeration*, 2004, 27 (1), 10-16.
- 438 [7] Darwish N.A., Al-Hashimi S.H., Al-Mansoori A.S. Performance analysis and evaluation  
439 of a commercial absorption-refrigeration water-ammonia (ARWA) system. *Int. J. of*  
440 *Refrigeration*, 2008, 31 (7), 1214-1223.
- 441 [8] Rossa J.A., Bazzo E. Thermodynamic modeling of an ammonia-water absorption system  
442 associated with a microturbine. *Int. J. of Thermodynamics*, 2009, 12 (1), 38-43.
- 443 [9] El May S., Boukholda I., Bellagi A. Modular simulation and thermodynamic analysis of  
444 absorption heat pumps. *Engineering with Computers*, 2010, 26 (2), pp. 185-192.
- 445 [10] El May S., Boukholda I., Bellagi A. Energetic and exergetic analysis of a commercial  
446 ammonia-water absorption chiller. *Int. J. of Exergy*, 2011, 8 (1), 33-50.

- 447 [11] Aspen Plus. Version 7.3.0.13 (25.0.4987), 2009. Aspen Technology, Inc., Ten Canal  
448 Park, Cambridge, MA, USA. [www.aspentech.com](http://www.aspentech.com).
- 449 [12] Duan Z., Moller N., Weare J.H. Equation of state for the NH<sub>3</sub>-H<sub>2</sub>O System. Journal of  
450 Solution Chemistry, 1996, 25 (1), 43-50.
- 451 [13] Renon H., Guillevic J.L., Richon D., Boston J., Britt H. A cubic equation of state  
452 representation of ammonia-water -liquid equilibrium data. Int. J. of Refrigeration, 1986, 9  
453 (2), 70-73.
- 454 [14] Vidal J. Equation of state – reworking the old forms. Fluid Phase Equilibria, 1983, 13  
455 (C), 15-33.
- 456 [15] Pátek J., Klomfar J. Simple functions for fast calculations of selected thermodynamic  
457 properties of the ammonia-water system. Int. J. of Refrigeration, 1995, 18 (4), 228-234.
- 458 [16] Tillner-Roth R., Friend D.G. A Helmholtz free energy formulation of the thermodynamic  
459 properties of the mixture {water+ammonia}. Journal of Physical and Chemical Reference  
460 Data, 1998, 27 (1), 63-77.
- 461 [17] Abovsky V. Thermodynamics of ammonia+water mixture. Fluid Phase Equilibria, 1996,  
462 116 (2), 170-176.
- 463 [18] Van Poolen L.J., Rainwater J.C. Critical-region model for bubble curves of ammonia-  
464 water with extrapolation to low pressures. Fluid Phase Equilibria, 1998, 150 (151), 451-  
465 458.
- 466 [19] Moshfeghian M., Shariat A., Maddox R.N. Prediction of refrigerant thermodynamic  
467 properties by equations of state: vapor liquid equilibrium behavior of binary mixtures.  
468 Fluid Phase Equilibria, 1992, 80 (C), 33-44.
- 469 [20] Weber L.A. Estimating the virial coefficients of the ammonia+water mixture. Fluid Phase  
470 Equilibria, 1999, 162 (1-2), 31-49.

- 471 [21]Barhoumi M., Snoussi A., Ben Ezzine N., Mejbri K., Bellagi A. Modeling of the  
472 thermodynamic properties of the ammonia/water mixture. *Int. J. of Refrigeration*, 2004,  
473 27 (3), 271-283.
- 474 [22]Schulz S.C.G. Equations of state for the system ammonia-water for use with computers.  
475 Proceedings of 13<sup>th</sup> International Congress of Refrigeration, Paper n° 2.06, pp. 431-436,  
476 Washington DC, 1971
- 477 [23]Ziegler B., Trepp Ch. Equation of state for ammonia-water mixtures. *Int. J. of*  
478 *Refrigeration*, 1984, 7 (2), pp. 101-106.
- 479 [24]Ruiter J.P. Simplified thermodynamic description of mixtures and solutions. *Int. J. of*  
480 *Refrigeration*, 1990, 13 (4), 223-236.
- 481 [25]Mejbri Kh., Bellagi A. Modeling of thermodynamic properties of the water-ammonia by  
482 three different approaches. *Int. J. of Refrigeration*, 2006, 29 (2), 211-218.
- 483 [26]Klein S.A. A model of the steady-state performance of an absorption heat pump. US  
484 Department of Commerce, National Bureau of Standards, National Engineering  
485 Laboratory, Center for Building Technology, NBSIR 82-2606, Washington DC, 1982.
- 486 [27]Poling, B.E., Prausnitz, J.M., O'Connell, J.P. *The properties of gases and liquids*. 5<sup>th</sup>  
487 Edition, McGraw-Hill, 2001.
- 488

489 **Table captions**

490 Table 1. Aspen-Plus thermodynamic property models tested

491 Table 2. Sum of squared errors for the regressed thermodynamic property models tested

492 Table 3. Interaction parameter  $k_{ij}$  for the considered cubic equations of state

493 Table 4. Calculation sequence of the chiller simulation

494 Table 5. Machine elements and their Aspen-Plus models with input data set

495 Table 6. Aspen-Plus model simulation results at a cooling air temperature of 35 °C

496 Table 7. Comparison between experimental data [26] and simulation results in terms of  
497 component heat duties and chiller *COP* at a cooling air temperature of 35 °C

498 Table 8. (*UA*) values of the heat exchangers calculated at a cooling air temperature of 35 °C

499 Table 9. Comparison between experimental temperature data [26], the simulation results of  
500 [10] and the model calculated temperatures at a cooling air temperature of 38 °C.

501

502

503

504  
505  
506  
507  
508  
509  
510  
511  
512  
513  
514  
515  
516  
517  
518  
519

Table 1. Aspen-Plus thermodynamic property models tested

<b>Aspen-Plus property model</b>	<b>Model name</b>
ENRTL-RK	Electrolyte NRTL/Redlich-Kwong
RKS-BM	Redlich-Kwong-Soave-Boston-Mathias
PENG-ROB	Standard Peng-Robinson
PR-MHV2	Modified Peng-Robinson-Huron-Vidal
PR-WS	Peng-Robinson-Wong-Sandler
NRTL-HOC	Non-Random-Two-Liquid/Hayden-O'Connell
SRK	Soave-Redlich-Kwong
WILS-RK	Wilson/Redlich-Kwong
PR-BM	Peng-Robinson-Boston-Mathias

Table 2. Sum of squared errors for the regressed thermodynamic property models tested.

<b>Aspen-Plus property model</b>	<b>Sum of squared errors</b>
PR-BM	36.55
PENG-ROB	38.36
WILS-RK	41.92
RKS-BM	44.86
SRK	45.07
ENRTL-RK	48.31
NRTL-HOC	53.00
PR-WS	80.42
PR-MHV2	226.62

520

521

Table 3. Interaction parameter  $k_{ij}$  for the considered cubic equations of state

522

Aspen-Plus property model	$k_{NH_3 H_2O}^{(1)}$ Default	$k_{NH_3 H_2O}^{(2)}$ Default	$k_{NH_3 H_2O}^{(3)}$ Default	$k_{NH_3 H_2O}^{(1)}$ Regressed	$k_{NH_3 H_2O}^{(2)}$ Regressed	$k_{NH_3 H_2O}^{(3)}$ Regressed
PR-BM	-0.3147	$1.4 \cdot 10^{-4}$	0	-1.0017	$1.1 \cdot 10^{-3}$	119.82
PENG-ROB	-0.2589	0	0	-1.0610	$1.2 \cdot 10^{-3}$	130.30
RKS-BM	-0.280	-0.280	0	-1.2146	$1.3 \cdot 10^{-3}$	162.214
SRK	0	$1.77 \cdot 10^{-5}$	0	-0.4246	$1.95 \cdot 10^{-4}$	26.492

523

524

525

Table 4. Calculation sequence of the chiller simulation

State point	Calculation step
1	Saturated liquid, composition, total mass flow and pressure
1A	Determined by the absorber model
2	Determined by the high pressure solution pump model
3	Determined by the solution valve 2 model
4	Determined by the pre-absorber model
5	Determined by the rectifier model
6	Determined by the generator model
7	Determined by the generator model
8	Determined by the condenser model
9	Determined by the refrigerant valve 1 model
10	Determined by the evaporator model
11	Determined by the vapor-liquid heat exchanger model
13	Determined by the vapor-liquid heat exchanger model
14	Determined by the pre-absorber model

526

Table 5. Machine elements and their Aspen-Plus models with input data set

Machine Element	Aspen Block	Input values
Condenser (COND)	Two-flow heat exchanger HEATX	Pinch temperature: Hot outlet-Cold inlet = 13.5 °C
Evaporator (EVAP)	Two-flow heat exchanger HEATX	Pinch temperature: Hot outlet-Cold inlet = 3 °C
Absorber (ABS)	Two-flow heat exchanger HEATX	Pinch temperature: Hot outlet-Cold inlet = 10.2 °C
Solution heat exchanger (SHX)	Two-flow heat exchanger HEATX	Pinch temperature: Hot outlet-Cold inlet = 16 °C
Expansion valve1 (DET1)	VALVE	Outlet pressure = 4.936 bar
Pre-absorber (PREAB)	FLASH block and HEATER block	Pressure = 4.936 bar Exit temperature = 76 °C
	MIXER	Pressure drop = 0 bar
Expansion valve2 (DET2)	VALVE	Outlet pressure = 4.936 bar
Generator (GEN)	RADFRAC	Reflux mass ratio = 0.09 Mass flow rate at the bottom = 55.06 kg/h
	HEATER	Pressure drop = 0 bar Exit temperature = 115°C
PUMP	PUMP	High pressure = 22.380 bar Isentropic efficiency = 1 <b>State point 1</b> <ul style="list-style-type: none"> <li>- Pressure = 4.936 bar</li> <li>- Temperature = 45.2°C</li> <li>- Total mass flow = 90.718 kg/h</li> <li>- Vapour fraction = 0</li> <li>- NH<sub>3</sub> Mass fraction = 0.437</li> <li>- H<sub>2</sub>O Mass fraction = 0.563</li> </ul>



530

531 Table 6. Aspen-Plus model simulation results at a cooling air temperature of 35 °C

State point	From	To	Pressure (bar)	Temperature (°C)	Vapour fraction	Mass flow rate (kg/h)	NH <sub>3</sub> Mass fraction (%)
1A	Absorber	Pump	4.936	45.2	0	90.718	43.7
2	Pump	Rectifier	22.380	46.6	0	90.718	43.7
3	DET2	PREAB12	4.936	115.3	0	55.060	9.0
4	PREAB2-2	Generator	22.380	108.1	0.006	90.718	43.7
5	Rectifier	PREAB2-2	22.380	64.3	0	90.718	43.7
6	EXCH	DET2	22.380	115.0	0	55.060	9.0
7	Generator	Condenser	22.380	105.6	1	35.658	97.0
8	Condenser	H-EXCH1	22.380	48.5	0	35.658	97.0
9	DET1	Evaporator	4.936	4.9	0.073	35.658	97.0
10	Evaporator	H-EXCH1	4.936	9.5	0.819	35.658	97.0
11	H-EXCH1	PREAB1-2	4.936	16.7	0.901	35.658	97.0
12	PREAB1-2	Mixer	4.936	76.0	1	22.425	94.8
13	H-EXCH1	DET1	22.380	24.0	0	35.658	97.0
14	Mixer	Absorber	4.936	76.0	0.254	90.718	43.7
15	PREAB1-2	Mixer	4.936	76.0	0	68.293	26.9
20	Generator	EXCH	22.380	192.6	0	55.060	9.0

532

533

534 Table 7. Comparison between experimental data [26] and simulation results in terms of  
 535 component heat duties and chiller *COP* at a cooling air temperature of 35 °C

<b>Parameter</b>	<b>Experimental value</b>	<b>Calculated value</b>
<i>Q</i> generator (kW)	17	15.91
<i>Q</i> evaporator (kW)	9.59	9.51
<i>Q</i> condenser (kW)	-	12.84
<i>Q</i> absorber (kW)	-	12.85
<i>COP</i>	0.56	0.59

536  
 537  
 538 Table 8. (*UA*) values of the heat exchangers calculated at a cooling air temperature of 35 °C

<b>Heat exchanger</b>	<b>[<i>UA</i>] (W/K)</b>
Condenser	390.0
Evaporator	3304.9
Absorber	630.0
H-EXCH1	55.9

539  
 540 Table 9. Comparison between experimental temperature data [26], the simulation results of  
 541 [10] and the model calculated temperatures at a cooling air temperature of 38 °C.

542

543

State points	Experimental data [26]	El May et al. [10]	Aspen-Plus simulation
	Temperature (°C)	Temperature (°C)	Temperature (°C)
1	52.6	50.9	47.4
2	51.6	51.2	47.3
3	119.7	128.3	120.2
4	111.9	109.6	107.6
5	70.4	68.8	65.1
7	113.9	119.4	104.7
8	53.1	49.9	55.2
9	7.1	5.2	5.5
10	11.3	8.5	8.2
11	24.3	13.3	13.1
13	16.4	29.6	28.2
14	76.9	86.0	77.0

544

545

546

547 **Figure captions**

548 Figure 1. Schematic representation of the absorption chiller

549 Figure 2.  $T$ - $x$ - $y$  VLE diagram at  $P = 2$  bar for ammonia/water mixture (predicted by models  
550 with default interaction parameters)

551 Figure 3.  $T$ - $x$ - $y$  VLE diagram at  $P = 10$  bar for ammonia/water mixture (predicted by models  
552 with default interaction parameters)

553 Figure 4.  $T$ - $x$ - $y$  VLE diagram at  $P = 25$  bar for ammonia/water mixture (predicted by models  
554 with default interaction parameters)

555 Figure 5.  $T$ - $x$ - $y$  VLE diagram at  $P = 2$  bar for ammonia/water mixture (predicted by models  
556 with regressed interaction parameters)

557 Figure 6.  $T$ - $x$ - $y$  VLE diagram at  $P = 10$  bar for ammonia/water mixture (predicted by models  
558 with regressed interaction parameters)

559 Figure 7.  $T$ - $x$ - $y$  VLE diagram at  $P = 25$  bar for ammonia/water mixture (predicted by models  
560 with regressed interaction parameters)

561 Figure 8. The absorption machine model in Aspen-Plus

562 Figure 9. Temperature comparison at different locations in the chiller at a cooling air  
563 temperature of 35 °C ( $UA$  values as output parameters of the model)

564 Figure 10. Temperature comparison at different locations in the chiller at a cooling air  
565 temperature of 26.7 °C ( $UA$  values as input parameters in the model)

566 Figure 11. Temperature comparison at different locations in the chiller at a cooling air  
567 temperature of 38 °C ( $UA$  values as input parameters of the model)

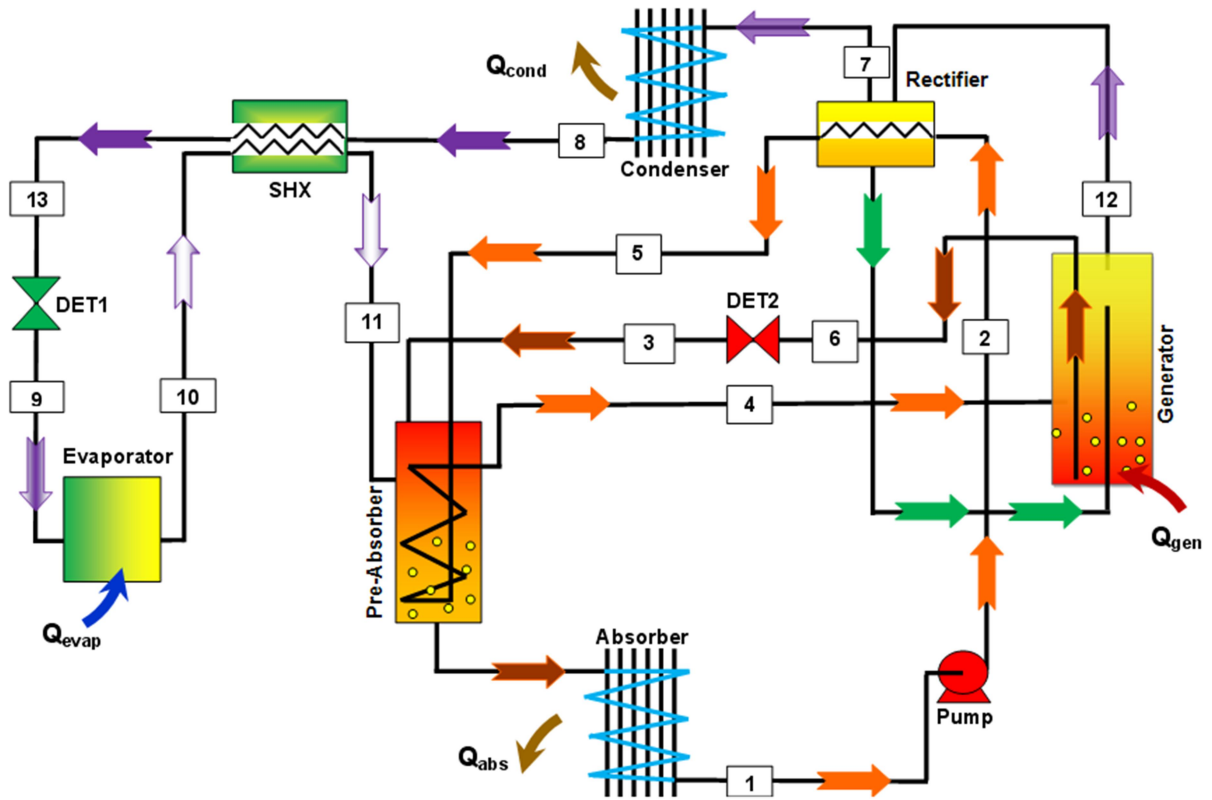
568 Figure12. Internal view of the commercial absorption chiller

569 Figure13. Schematic representation of the main components of the absorption chiller

570

571

572



573

574

Figure1. Schematic representation of the absorption chiller

575

576

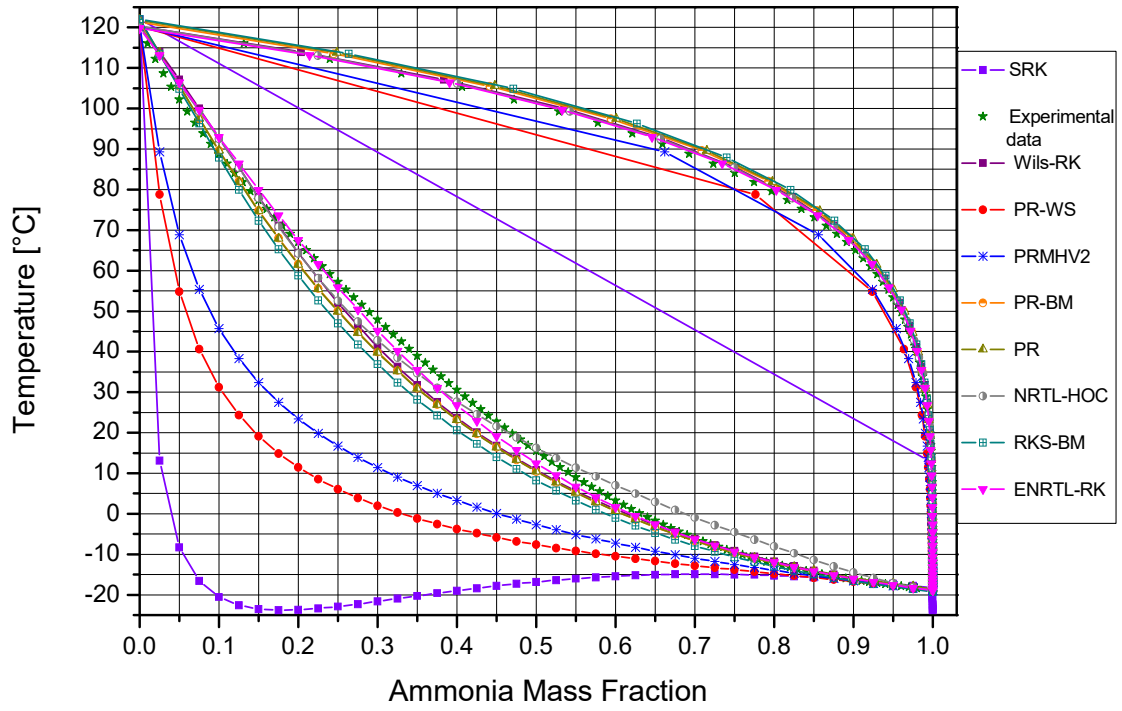
577

578

579

580

581



582

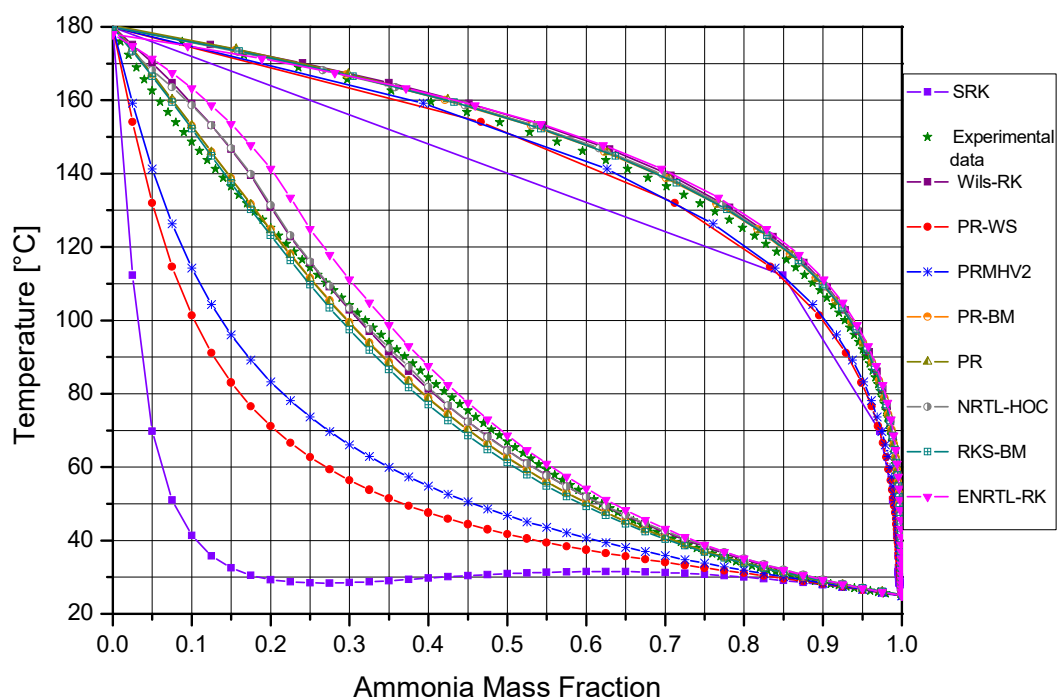
583

Figure 2.  $T$ - $x$ - $y$  VLE diagram at  $P = 2$  bar for ammonia/water mixture (predicted by models with default interaction parameters)

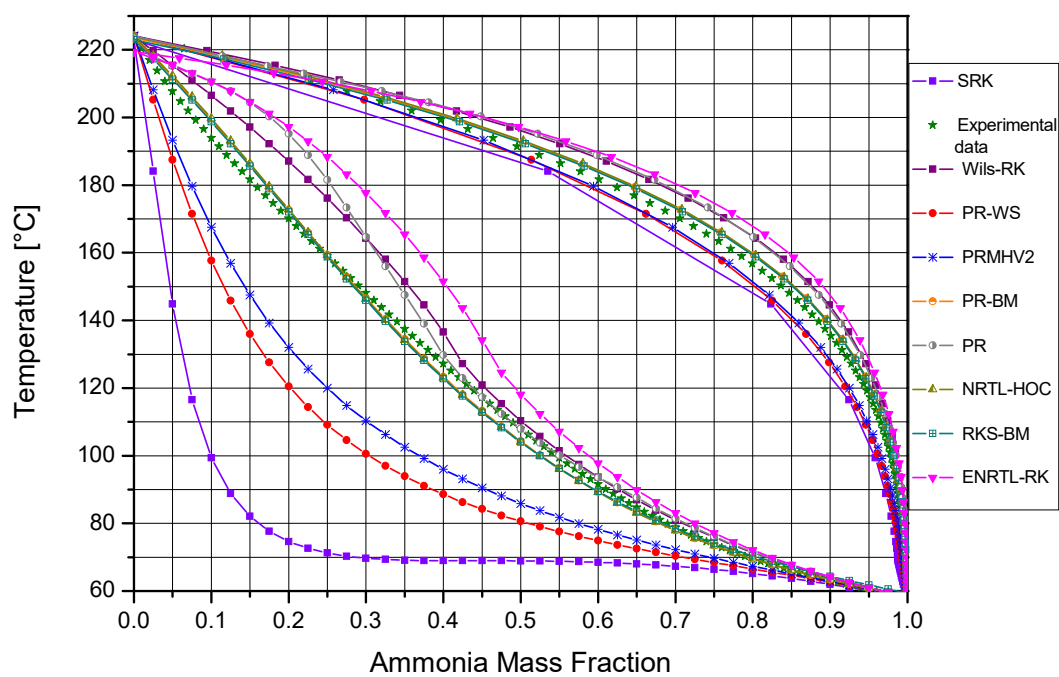
584

585

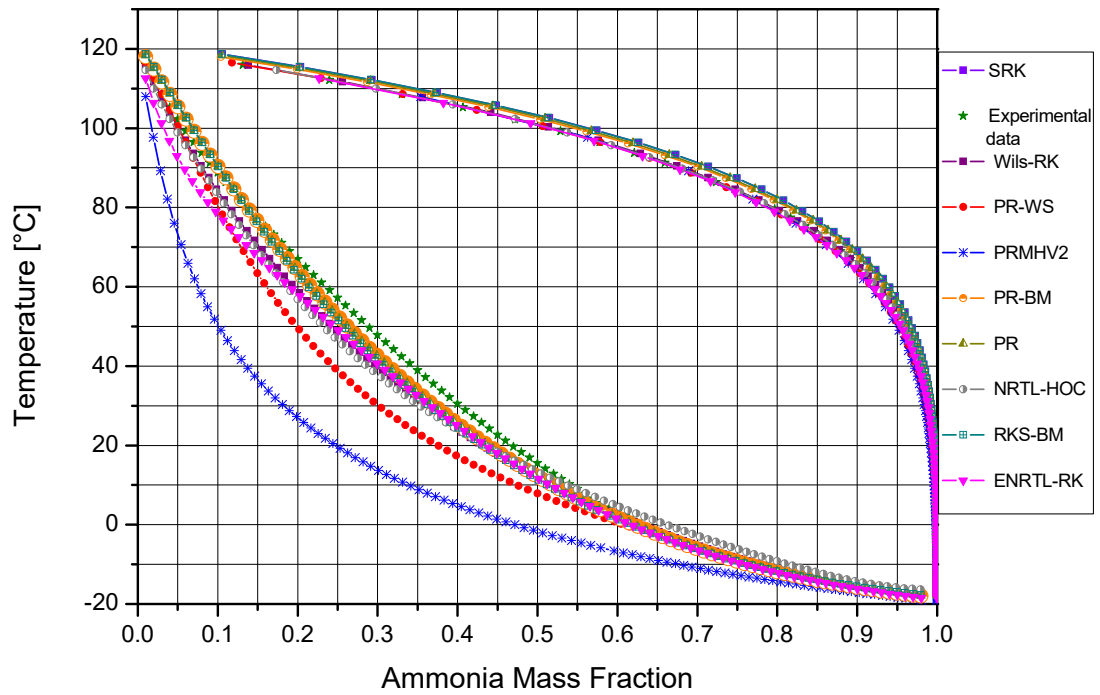
586



587  
 588 Figure 3.  $T$ - $x$ - $y$  VLE diagram at  $P = 10$  bar for ammonia/water mixture (predicted by models  
 589 with default interaction parameters)



590  
 591 Figure 4.  $T$ - $x$ - $y$  VLE diagram at  $P = 25$  bar for ammonia/water mixture (predicted by models  
 592 with default interaction parameters)

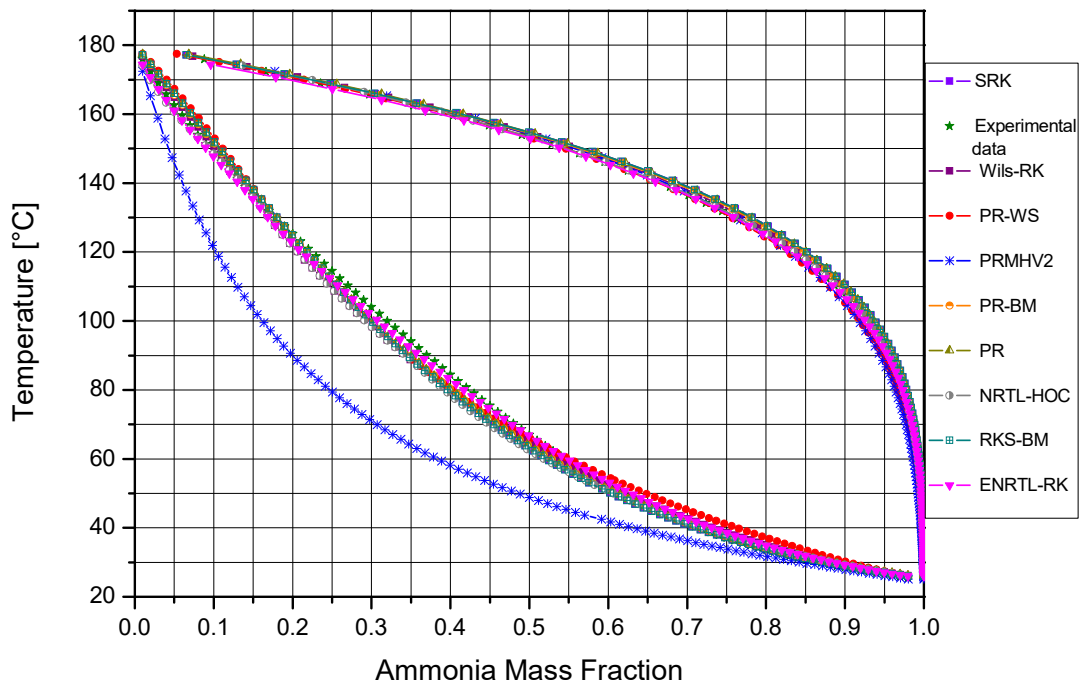


594

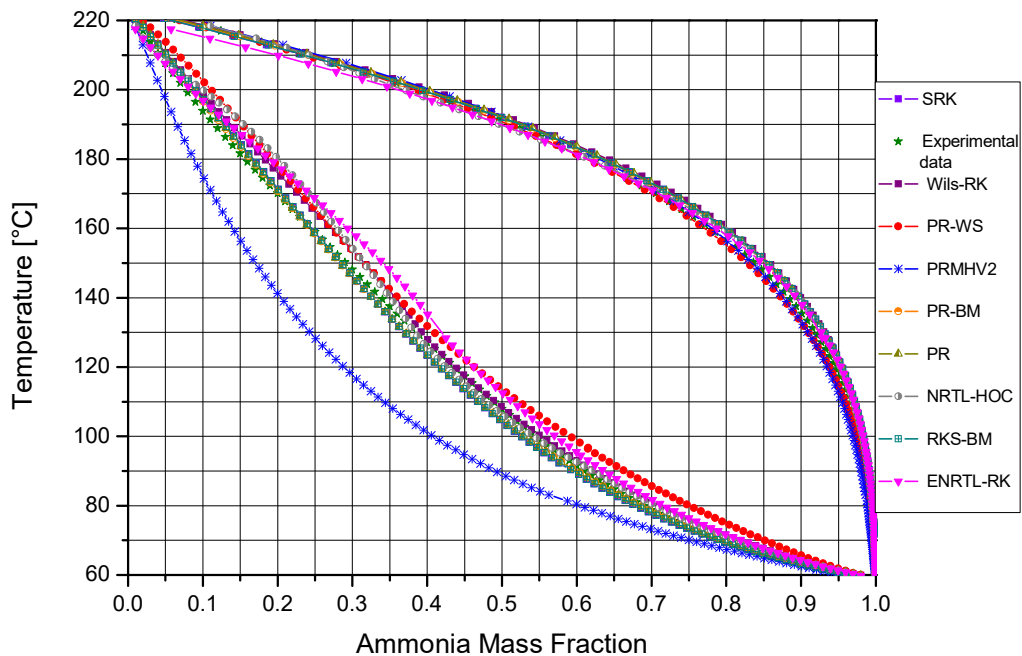
595

Figure 5.  $T$ - $x$ - $y$  VLE diagram at  $P = 2$  bar for ammonia/water mixture (predicted by models with regressed interaction parameters)

596

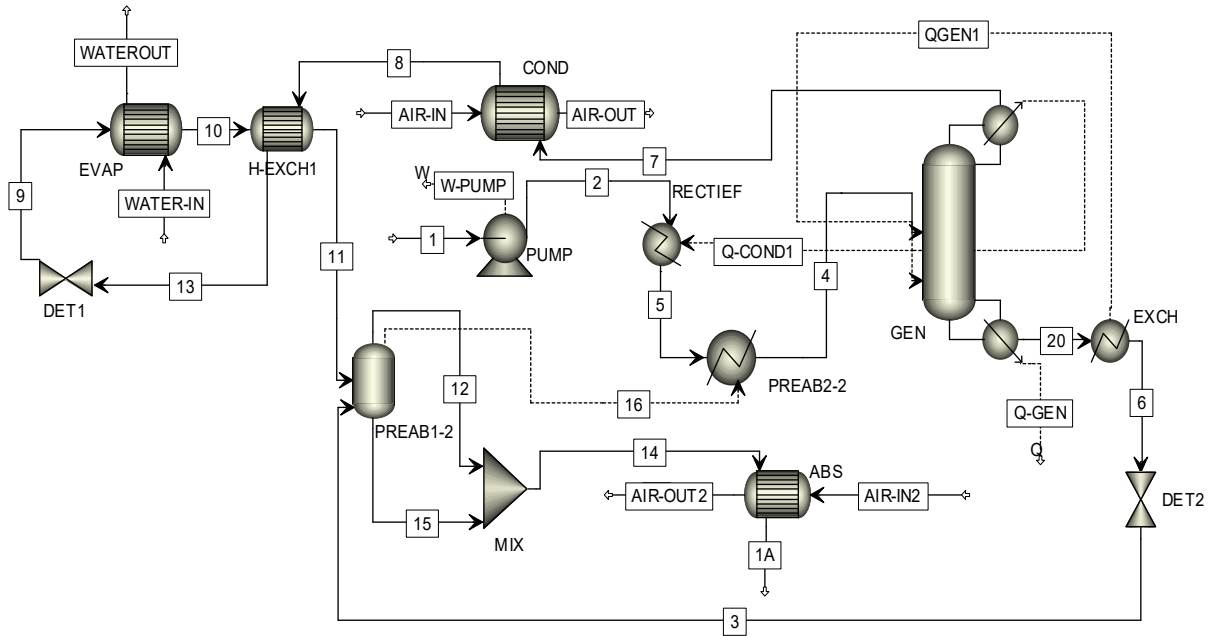


597  
 598 Figure 6.  $T$ - $x$ - $y$  VLE diagram at  $P = 10$  bar for ammonia/water mixture (predicted by models  
 599 with regressed interaction parameters)



600  
 601 Figure 7.  $T$ - $x$ - $y$  VLE diagram at  $P = 25$  bar for ammonia/water mixture (predicted by models  
 602 with regressed interaction parameters)

603



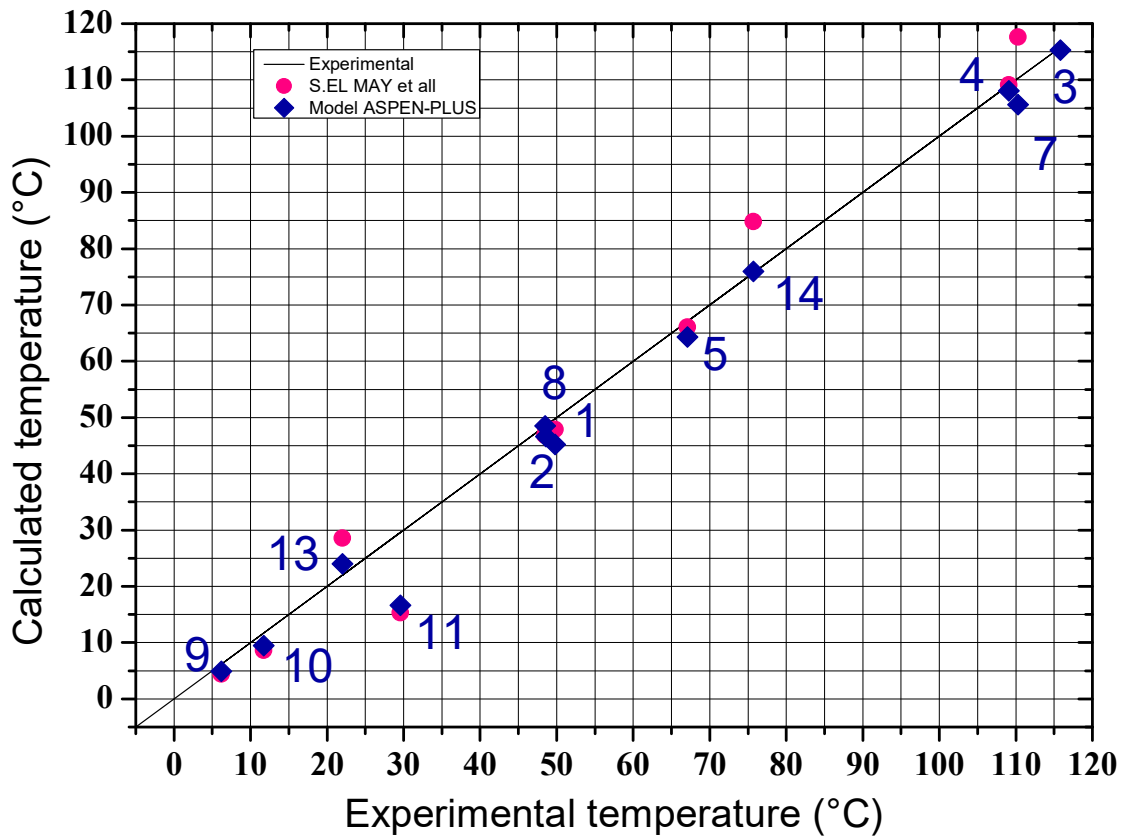
604

605

Figure 8. The absorption machine model in Aspen-Plus

606

607

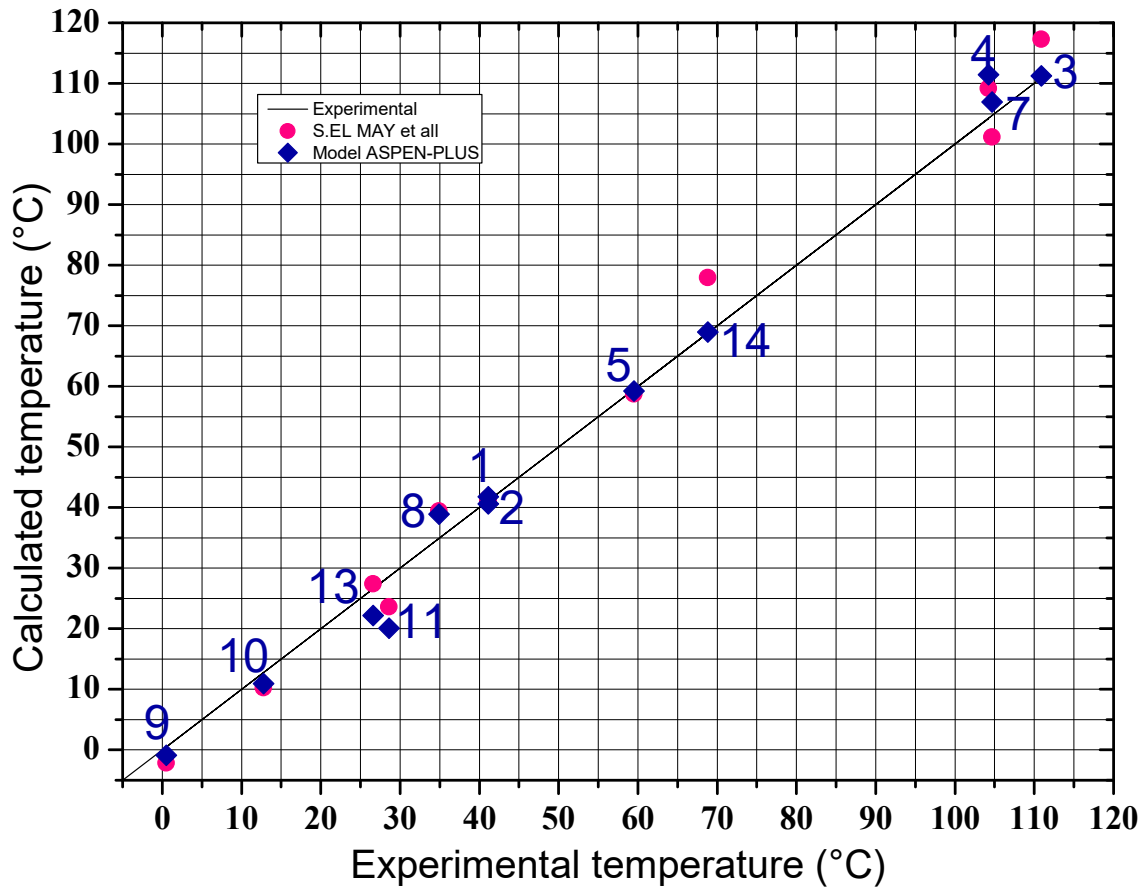


608

609 Figure 9. Temperature comparison at different locations in the chiller at a cooling air  
610 temperature of 35 °C (*UA* values as output parameters of the model)

611

612

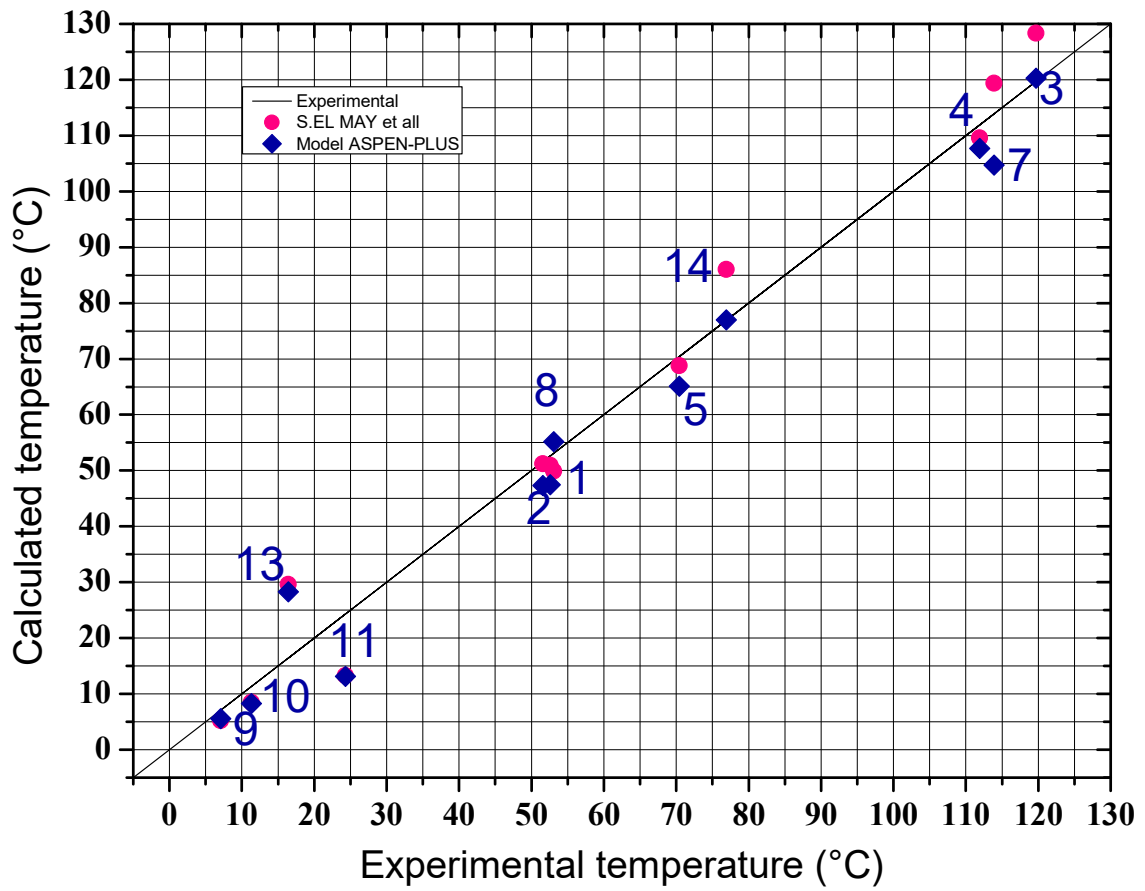


613

614 Figure 10. Temperature comparison at different locations in the chiller at a cooling air  
615 temperature of 26.7 °C (*UA* values as input parameters in the model)

616

617



618

619 Figure 11. Temperature comparison at different locations in the chiller at a cooling air  
620 temperature of 38 °C (*UA* values as input parameters in the model)